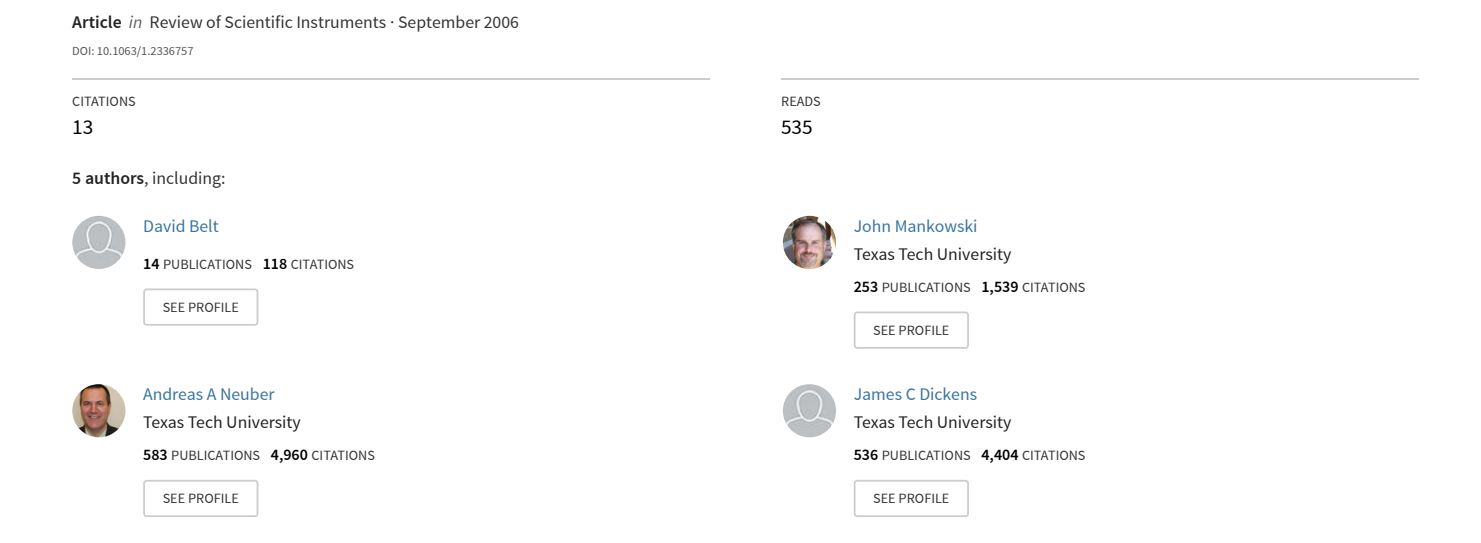
Design and implementation of a flux compression generator nonexplosive test bed for electroexplosive fuses





Design and implementation of a flux compression generator nonexplosive test bed for electroexplosive fuses

D. Belt, J. Mankowski, A. Neuber, J. Dickens, and M. Kristiansen

Citation: Review of Scientific Instruments 77, 094702 (2006); doi: 10.1063/1.2336757

View online: http://dx.doi.org/10.1063/1.2336757

View Table of Contents: http://scitation.aip.org/content/aip/journal/rsi/77/9?ver=pdfcov

Published by the AIP Publishing

Articles you may be interested in

Fast modeling of flux trapping cascaded explosively driven magnetic flux compression generators

Rev. Sci. Instrum. 84, 014703 (2013); 10.1063/1.4775488

The advanced helical generator

Rev. Sci. Instrum. 81, 034701 (2010); 10.1063/1.3309788

Electric discharge caused by expanding armatures in flux compression generators

Appl. Phys. Lett. 94, 171502 (2009); 10.1063/1.3127525

Fast-charging compact seed source for magnetic flux compression generators

Rev. Sci. Instrum. 79, 124702 (2008); 10.1063/1.3046280

ECF2: A pulsed power generator based on magnetic flux compression for Kshell radiation production

AIP Conf. Proc. 651, 51 (2002); 10.1063/1.1531279



Design and implementation of a flux compression generator nonexplosive test bed for electroexplosive fuses

D. Belt, J. Mankowski, A. Neuber, J. Dickens, and M. Kristiansen Center for Pulsed Power and Power Electronics, Texas Tech University, Lubbock, Texas 79409-3102; Departments of Electrical, Texas Tech University, Lubbock, Texas 79409-3102; and Computer Engineering and Physics, Texas Tech University, Lubbock, Texas 79409-3102

(Received 25 May 2005; accepted 23 July 2006; published online 19 September 2006)

Helical flux compression generators (HFCGs) of a 50 mm form factor have been shown to produce output energies on the order of ten times the seeded value and a typical deposited energy of 3 kJ into a 3 μ H inductor. By utilizing an electroexplosive fuse, a large dI/dt into a coupled load is possible. Our previous work with a nonoptimized fuse has produced ~ 100 kV into a 15 Ω load, which leads into a regime relevant for high power microwave systems. It is expected that ~ 300 kV can be achieved with the present two-stage HFCG driving an inductive storage system with electroexploding fuse. In order to optimize the electroexplosive wire fuse, we have constructed a nonexplosive test bed which simulates the HFCG output with high accuracy. We have designed and implemented a capacitor based, magnetic switching scheme to generate the near exponential rise of the HFCG. The varying inductance approach utilizes four stages of inductance change and is based upon a piecewise linear regression model of the HFCG wave form. The nonexplosive test bed will provide a more efficient method of component testing and has demonstrated positive initial fuse results. By utilizing the nonexplosive test bed, we hope to reduce the physical size of the inductive energy storage system and fuse substantially. © 2006 American Institute of Physics.

[DOI: 10.1063/1.2336757]

I. INTRODUCTION

Helical flux compression generators (HFCGs) have a specific energy density that is superior to capacitive driven pulsed power sources. However, to make a HFCG source practical, the output pulse needs to be conditioned such that the source will be better matched to a typical pulsed power load. A small HFCG unit usually produces several hundreds of kiloamperes but only at a few tens of kilovolts voltage level. Previously, we have studied the experimental performance of small (50 mm diameter and below) HFCGs, including computer modeling of flux and Ohmic losses.² For a HFCG unit to be relevant to high power microwave (HPM) and electron beam devices, an inductive energy storage system is usually utilized to produce the several hundreds of kilovolts that are needed to drive such a system.³ The typical inductive energy storage system utilizes an electroexplosive fuse which allows a large dI/dt, up to 10^{13} Å/s , into a coupled load.4,5

One present task that exists is the optimization of the electroexplosive fuse for the HFCG unit. Previous optimization attempts were made by utilizing the HFCG units directly, which is a time and cost consuming approach due to the true one-shot nature of explosive devices, in general. In order to have a reliable repetitive source for the evaluation of the electroexplosive fuse a nonexplosive test bed was designed and constructed. The output current of the nonexplosive test bed system mimics the output of a 45 kA HFCG unit. It should be noted that simply discharging a capacitor (bank) into the energy storage inductance leads to a current wave form that exhibits the highest dI/dt at small current

amplitudes rather than at high current amplitudes as observed for a HFCG driven storage inductance (quasiexponential current rise). Hence, the test bed was designed to utilize a system of capacitors and magnetically switched inductances, which produced the quasiexponential rise of the current output wave form. In order to match this exponential rise, a technique of switching inductors sequentially into parallel has been developed.

We will discuss the design, construction, and observed behavior of the nonexplosive test bed and give details on the employed sequential magnetic switching.

II. DESIGN

The design of the switching inductance system is based on polynomial regression of the output wave form of the HFCG unit. We chose as our test bed design goal a typical second stage output current wave form of a dual stage HFCG, which had a rise time of 7.5 μ s and can be compared to an exponential slope. Particularly, there are four stages in the model, and the slope of each stage is the equivalent of a *RLC* discharge curve, see Fig. 3. The mathematical model allowed the calculation of the inductance value for each stage. Table I lists the inductance per stage and the equivalent parallel combination during each stage of the model. The final inductance of the system is equivalent to 1.3 μ H and is considered the equivalent load of the system. This inductor value is somewhat lower but still typical for an energy storage inductor utilized in our previous HFCG experiments.

The desired result of the system is to have maximum output current with minimal charging voltage and a current

TABLE I. Inductance per stage (L) and equivalent load inductance per stage (L load), cf. Fig. 3. The equivalent dI/dt for each stage derived from modeling.

Stage No.	C (μF)	$R \pmod{\mathrm{m}\Omega}$	$L \ (\mu { m H})$	L load $(\mu { m H})$	dI/dt kA/μs
1	3.72	160	20	20	3.4
2	3.72	160	17	9.3	1.6
3	3.72	160	8	3	1
4	3.72	160	0.55	1	0.6

rise time corresponding to the HFCG unit. An overall system diagram can be seen in Fig. 1 where the design and construction begin with the pulse forming network (PFN) system.

The equivalent series resistance (ESR) and equivalent series inductance (ESL) values of the capacitors were measured by a direct short discharge and allowed accurate modeling of the capacitors. The capacitors used (Aerovox PX300D25) have an ESL value of 250 nH and an ESR value of 4 m Ω at the relevant frequencies. Through PSPICE circuit simulation, the best possible combination of load inductance and capacitance with an examination of charging voltage, peak output current, and output rise time is determined. The system block diagram can be seen in Fig. 1, where the PFN's capacitors are charged to a preset voltage before the spark gap (SG) is closed. When the PFN discharges, the magnetic switching (MS) scheme (inductors) is utilized for pulse shaping. The fuse begins energy absorption and opens up when the deposited energy reaches the fuse's blow limit.^{3,4} The peaking gap (PG) isolates the HPM equivalent load (load) until the gap's breakdown voltage is reached across the inductors. The voltage probes (V probes 1 and 2) give a differential voltage measurement across the load, and a Rogowski coil measures the current through the load. The diode pack is utilized in case the fuse fails to open and prevent ringing. The R1 resistor helps to improve commutation of the diode pack and also improves PFN impedance matching.

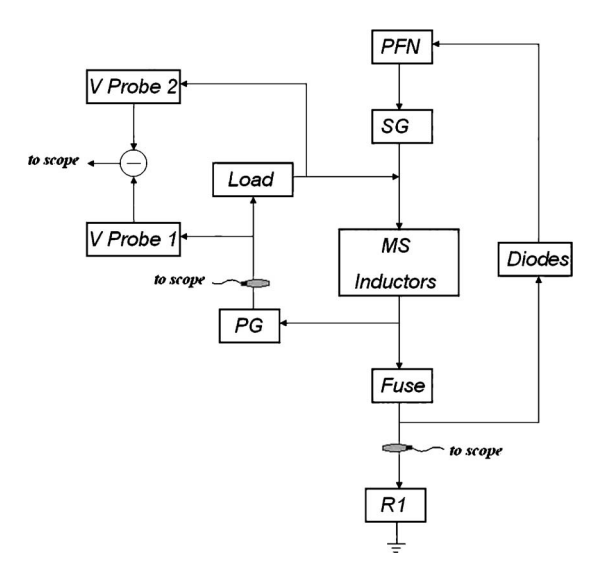


FIG. 1. Block diagram for the overall system of the nonexplosive test bed.

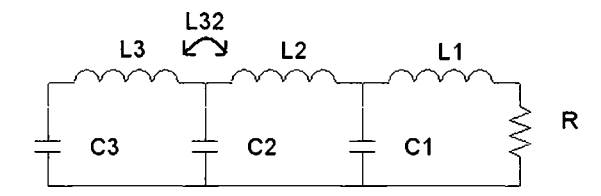


FIG. 2. Typical type E PFN (three stage) schematic with single tapped inductor

A. Pulse forming network

The nonexplosive test bed utilizes a capacitive energy storage system, a type E PFN, into which the switching inductance technique is integrated. The PFN system is designed for maximum current output (minimal load impedance) with the appropriate rise time (Fig. 2). For testing purposes, a 1.3 µH air core inductor is substituted in place of the switching inductance scheme. The output of the PFN with this constant inductance load is designed to match the final stage model of the HFCG wave form since the system will have this equivalent load inductance value at this point. In Fig. 3, PFN output matched the final stage model of the HFCG wave form. The PFN utilizes a 4 μ s rise time (0%– 90%), and the magnetic switching scheme will be added to shape the initial rise to give the total 7.5 μ s rise time. The PFN is composed of seven 1.86 μ F capacitors with two capacitors in parallel on the first and second banks, and three capacitors in parallel on the third bank. The fundamental bank employs the switching inductance scheme as the load inductance while the second bank utilizes a 650 nH inductor (L2) and the third stage utilizes a 700 nH inductor (L3). Inductors L2 and L3 are constructed from a single inductor tapped off to the correct values, thus experience mutual magnetic coupling of 15% (L32).

To achieve the maximum current output possible, the PFN is purposely mismatched into a minimal load resistance, usually around 200 m Ω , where the correct matching impedance is 1.67 Ω . The mismatched impedance combined with the large fundamental inductance value results in a rounded top on the PFN output. A large load inductance value is desired for testing the inductive energy storage method used with the fuse.

Typically it is detrimental to the lifetime of oil-filled capacitors to have voltage ringing beyond 60% of the charg-

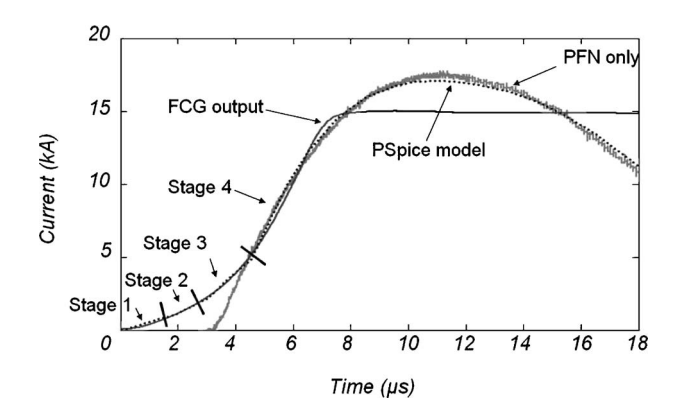


FIG. 3. Initial design of changing inductance load through stages along with the PFN output matched to the final 1.3 μ H load.

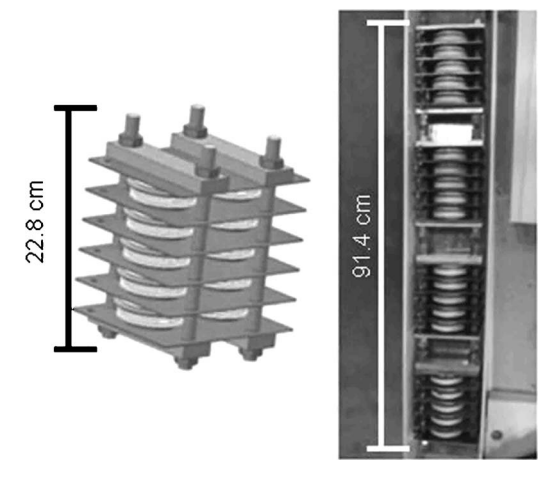


FIG. 4. Freewheeling diode assembly; left: single diode pack drawing (two parallel, five series diodes); right: Image of final assembly consisting of four packs.

ing voltage and, as a solution, a free wheeling diode assembly is utilized in the PFN system. The International Rectifier diodes used are rated to 1.8 kV and 10 kA (at 1 ms). The diodes are placed in two parallel stacks of 20 series diodes in order to achieve a voltage rating of 36 kV. A single diode pack along with all four packs assembled can be seen in Fig. 4. The diode assembly is stress tested with the PFN and under the short pulse length conditions (maximum of $500~\mu s$) is able to support a preratable output current of 50~kA.

The capacitance of the diodes and the added inductance introduced by the connections create a conduction delay, dampening the benefit of the diode assembly. Due to the physical size of the components and the connection lengths it is difficult to reduce these parasitic values. By placing a balancing resistor (R1=0.16 Ω , see Fig. 1) between ground and the output of the system/diode connection, the commutation of the diode assembly is improved dramatically. As a secondary factor, the impedance match of the PFN is improved which also reduces voltage ringing. Overall, the diode assembly reduces voltage ringing from 98% to 35%. Ceramic composite resistors (HVR W1528AR16J) are used due to the high and abrupt energy densities produced where typical carbon composite resistors failed. The resistors have an energy rating of 110 kJ, measure 152 mm in diameter, and a 25.4 mm thickness with a pulsed voltage rating of 28 kV in air. To prevent surface flashover across the resistor, it is placed in a container capable of either fluid insulators or pressurized gases (up to 60 psi), see Fig. 5. During typical operation, the container is pressurized to 40 psi with compressed air. The outer casing is constructed of 1.27 cm thick Lexan tube and is 31 cm tall. The added length allows the possibility of a series stack of resistors to be used without modification. Both ends are sealed with rubber o-ring gaskets and are bolted together using 1.27 cm diameter all-thread rods.

B. Magnetic switch

In order for the application of the inductive switching scheme to be successful, a reliable switching method must be

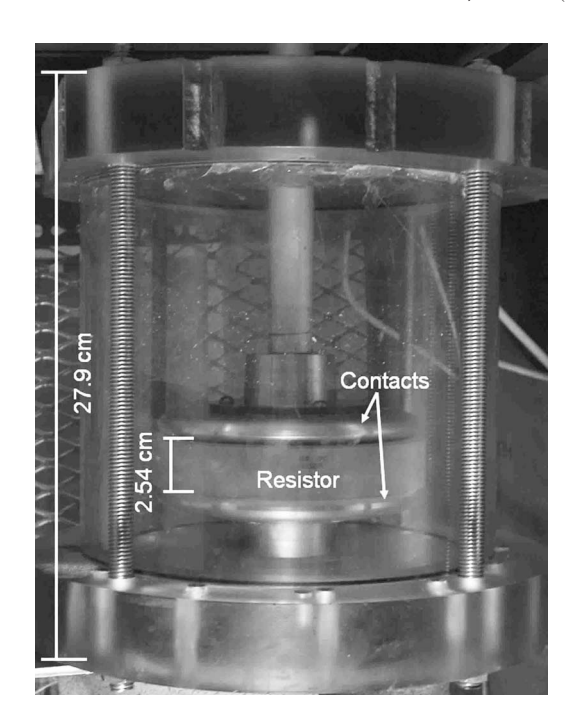


FIG. 5. Power resistor encasement/assembly, cf. R1 in Fig. 1. Operating pressure, 40 psi air typically.

implemented. Several approaches were examined including spark gaps, integrated gate bipolar transistors (IGBTs), and silicon controlled rectifiers (SCRs). Since the system would operate at voltages at 10 kV and above, IGBT and SCR units would be costly, and the reliability/accuracy of self-triggered multiple spark gaps is low, a different switching method had to be implemented. The magnetic switching technique became a viable option since the switching is based upon the saturation point of the core material. The operation of the magnetic switch involves changing from a very high inductance value to a low inductance value upon saturation. Upon full core saturation, the inductance value is equivalent to the air core inductance of the windings around the core.

In order to achieve a low core saturated inductance value, copper conductor strips with a width ranging from 22.2 to 31.75 mm (depending upon the core utilized) and a thickness of 0.5 mm were used. By using wide conductors as windings, the ESL value in the saturated state is significantly reduced. Since the magnetic switches will be in series after switching, a parallel-series inductor combination is established and the entire inductor circuit must be equivalent to the previously stated load inductance of 1.3 μ H. Figure 6 displays the parallel-series combination along with the inductance values established by the magnetic switches after

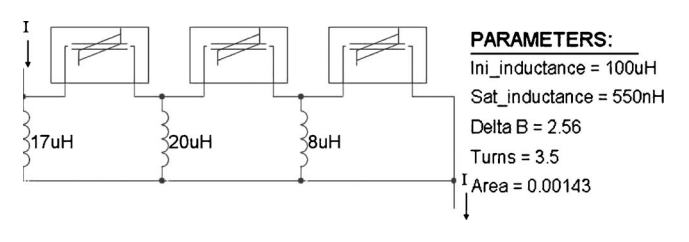


FIG. 6. PSPICE representation of inductance changing circuit (initial simulations)

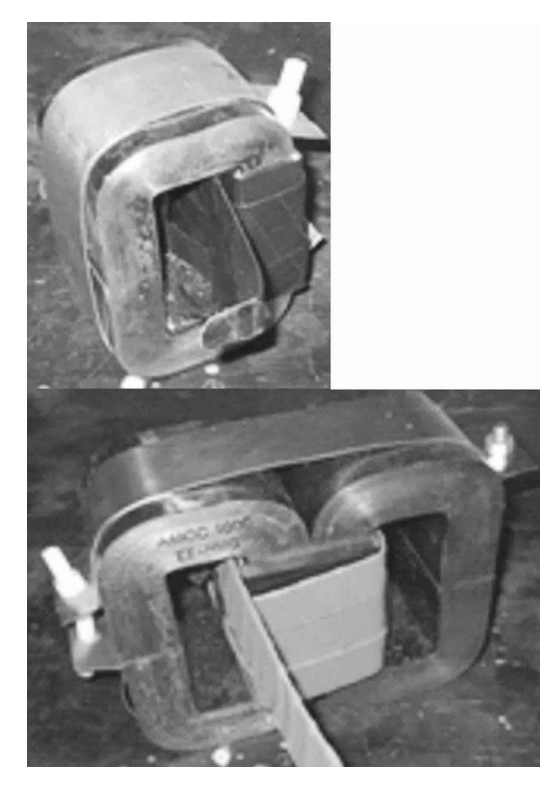


FIG. 7. Magnetic switch assemblies (saturable inductors) for 15 and 45 kA output. AMCC 630 (7.6 cm wide and 12.7 cm tall) and doubled AMCC 1000 (21.5 cm wide and 17.7 cm tall)

saturation. The typical unsaturated inductance is in the $100~\mu\mathrm{H}$ regime.

For simplicity, the magnetic switches are designed to have the same saturated inductance value. By calculation of series-parallel combination (circuital analysis with one unknown), the saturated core inductance must be equivalent to 550 nH. The strip width was chosen to achieve this value while having negligible fringing effects that would still allow proper core coupling. Due to the width of the copper conductors, the maximum number of turns around the core is reduced to $3\frac{1}{2}$ turns. For insulation purposes, the copper conductors are wrapped in electrical insulation tape, followed by two layers of self-fusing silicon rubber insulation tape (McMaster: 7643A46) rated to 8 kV per single layer. The assembled magnetic switches for the 15 kA (top) and the 45 kA (bottom) are shown in Fig. 7 below. The magnetic cores are constrained together using a stainless steel strap and nylon all-thread rods/nuts.

Based upon the given properties of the core material and the number of windings, the time at which saturation of the core occurs can be calculated using the flux density equation,

$$\Delta B = \frac{1}{NA} \int_0^{\tau} V(t)dt,\tag{1}$$

where N is the number of turns on the core, A is the core's cross sectional area, V(t) is the voltage across the inductor, and τ is the voltage applied time in seconds. The change in flux density (ΔB) relationship to the hysteresis curve of the material can be seen in Fig 8. For the material used (Metglas® 2605SA1), the saturation flux density value (B_s) is 1.56 T while the retentivity (B_r) value is 1.03 T. The mag-

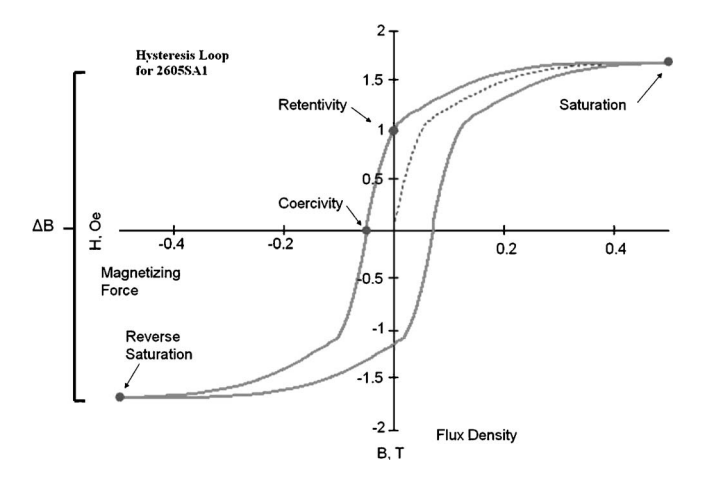


FIG. 8. Hysteresis loop for the 2605SA1 material used.

netic switching system was designed with the intent of operating from the reverse saturation point to full forward saturation. The system is designed to prevent reverse current conduction through the cores, meaning the cores should relax to the retentivity point of the hysteresis curve. To start the cores in reverse saturation, the physical connections are designed for quick release and allow the cores to be rotated 180° after every shot. Due to the sharp curvature of the hysteresis curve, only a couple of 10 ns are added to the saturation time of the magnetic switch.

Since the system was designed to operate at multiple output currents (15 and 45 kA), multiple core sizes are used. For fuse testing at the 15 kA level, the AMCC 630 cores with a cross sectional area of 14.3 cm² are implemented. With an applied voltage of 10 kV across the magnetic switch, the saturation time is 1.84 μ s, according to the flux density equation. For fuse testing at the 45 kA output level, the AMCC 1000 cores are implemented. Since the charging voltage of the system increased by a factor of 3 (30 kV) the saturation time of one AMCC 1000 core was insufficient and by doubling the cores, the correct time is achieved. For the AMCC 1000 cores with a cross sectional area of 46 cm² (2 \times 23 cm²) and an applied voltage of 32 kV, the saturation time is 1.80 μ s.

C. Fuse interface

In order to properly design the electroexplosive fuse for a HFCG unit, an equivalent HPM load was constructed from a large volume water resistor (Fig. 9). The cupric sulfate (CuSO₄) water resistor is constructed from a 7.62 cm inner diameter Lexan tube, with a length of 25.4 cm between conductors, and has a final resistance of 16.3 Ω . Typically to achieve a resistance value this low requires a high concentration of cupric sulfate but the solution usually becomes insoluble after a certain concentration. By physically increasing the cross sectional area of the resistor, less cupric sulfate is needed to achieve the desired resistance. For final load simulation, an adjustable peaking gap is introduced to couple in the HPM source equivalent load at the proper voltage. The breakdown of the peaking gap is dependent upon the voltage gain from the utilization of the electroexplosive fuse. The peaking gap is problematic due to the breakdown being

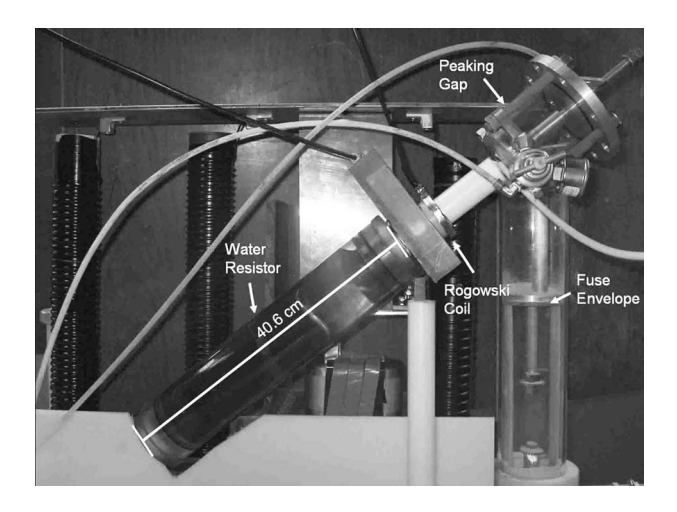


FIG. 9. Water resistor (HPM Load) and peaking gap. Optimal gap distance is 2 mm at 25 psi of $\rm N_2$ gas.

highly dependent upon the atmospheric conditions at the time of testing. For this purpose, the gap is filled with a constant pressure of nitrogen (N_2) gas. Another problem is the accuracy of gap spacing and the effect upon forward and reverse conductions through the load. If the gap is set too small, the long pulse length (7.5 μ s) of the initial discharge will cause the coupling gap to break down. If the gap distance is set too large, the high voltage pulse with shorter rise time (<100 ns) generated by the inductive energy storage system will not break down the gap. For accurate peaking gap control, a closely optimized gap distance is established (2 mm) and fine-tuning is controlled by pressure adjustment of the nitrogen (typically 25 PSIG).

The fuse envelope is designed for optimization of various factors including different quenching media, an easily adjustable fuse length, and rapid fuse construction. The envelope is sealable for use with solid, liquid, or gas quenching media, and an adjustable all-thread center allows fuse length adjustability without constructing new connections, see Fig. 10. Typically, glass impact beads [Grainger No. 2W580/ Ballotini No. AD (70-140)] were used as the quenching media during fuse testing.

The final assembled test bed is significantly large in comparison with the HFCG unit. The test bed occupies a space of 2.4 m (8 ft) length by a 1.2 m (4 ft) width by a 1.7 m (5.5 ft) height, where the HFCG has a 50 mm in-bore diameter and a typical length of 30 cm. Majority of the size of the test bed is a result of the physically large capacitors used. This is to be expected since the energy storage density of a HFCG is much larger than a capacitor.

D. PSPICE

Developing a PSPICE model of the nonexplosive test bed enables evaluating the system's performance. By determining the parasitic inductance and resistance values, the test bed was fully analyzed. The PSPICE model along with the matching wave forms can be seen in Figs. 11 and 12. The magnetic switching circuit is a PSPICE representation of the flux density equation calculation previously discussed. The model accounts for the v s applied to the switch along with



FIG. 10. Fuse geometry; Left: drawing of fuse holder; Right: photograph of the constructed fuse.

the number of turns and the cross sectional area of the core material. Based on this, the PSPICE model is used to optimize the output as seen in Fig. 12 through magnetic switching adjustments. In conjunction with the test bed PSPICE model, we are able to construct a realistic fuse model based upon previous fuse performance and development to estimate the initial results of the system. After improving/decreasing the parasitic inductance from the fuse and connections, the per-

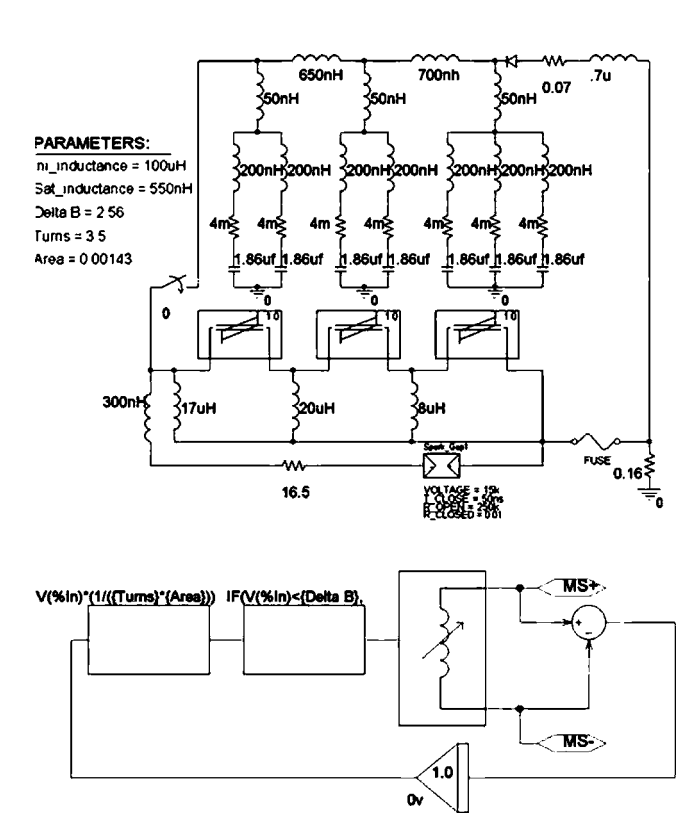


FIG. 11. Final circuit for the nonexplosive test bed with HPM equivalent load and peaking gap (PSPICE model). Magnetic switch PSPICE implementation circuit.

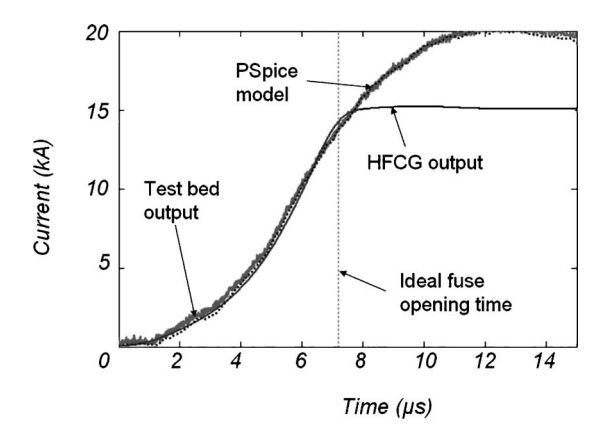


FIG. 12. Finalized test bed output with matching PSPICE model. Ideal fuse opening time designated at 7.3 μ s.

formance increased dramatically to closely match the initial PSPICE model with minor deviations. The initial fuse model will then be used to simulate results at higher currents.

III. TESTING

The overall system is broken down into subsystems, which are tested individually, integrated into the system, and then tested again within the final assembly. By testing components individually, any discrepancies from the initial design can be found and the component redesigned for optimal operation. These discrepancies are usually a result of poor connection style or unforeseen component parasitics. Another benefit of this approach is the ability to compare the mathematical models and the PSPICE models to the experimental system. The first subsystem in testing is the PFN, followed by the magnetic switching scheme integration. The PFN model comparison yielded the a priori unknown parasitic values that are present in the capacitors, connections, and the spark gaps used. Performance improvements are achieved by utilizing a stripline connection method for the capacitors, using copper connections in place of aluminum connections, and by correct component placement for overall system size reduction. The PFN system tested without the magnetic switching scheme yielded an output of 53 kA at a charging voltage of 30 kV. After the magnetic switching scheme is introduced, the series resistance of the inductors decreases the output to 50 kA at a charging voltage of 35 kV. This charging voltage is approaching an unsafe operating range due to the voltage ringing still present. For this reason, the maximum output of the system is declared at 45 kA at a 30 kV charging voltage.

The initial magnetic switching regime is tested with a single capacitor to establish core performance analysis. Once the proper number of turns and core size is established, the switches are integrated into the system. Various core sizes of the 2605SA1 material class were tested and resulted in holdoff times of 500 ns (AMCC 125) to a maximum of 3.5 μ s (AMCC 1000) at a voltage of 10 kV. The final system integration consisted of the HPM equivalent load (16.3 Ω) and peaking gap which was tested with an initial fuse design. The

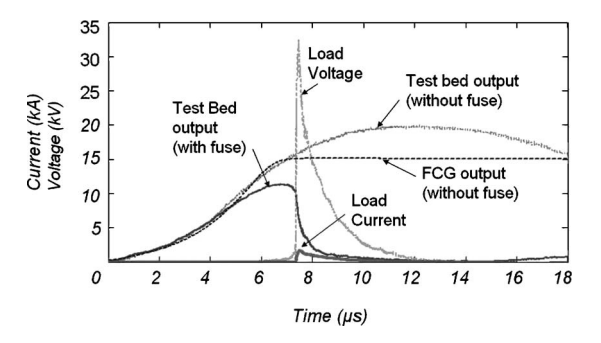


FIG. 13. Final (optimized) output of the nonexplosive test bed and initial fuse results with an optimal peaking gap. Maximum dI/dt at 15 kA test bed output is 2×10^{10} A/s.

load current along with the peak load voltage is measured by a Rogowski coil and a Pulsar (resistance divider) high voltage probe. The peaking gap is adjusted to achieve the maximum coupling voltage possible while not limiting the rise time.

Since the fuse is designed to open at the peak time of the HFCG current output (7.3 μ s), only the rise curvature is relevant for fuse testing. For this reason, the wave form matches after 7.5 μ s is disregarded and deemed unnecessary. Once the fuse completely opens, the test bed capacitors will have a residual charge which will be discharged by a mechanical switch.

The initial results of fuse testing are shown in Fig. 13. Due to the properties of fuse operation, the resistance increases as Ohmic heating occurs within the fuse material. This increase in resistance causes the reduction of output current seen by the test bed output with a fuse versus the test bed output without a fuse. Utilizing the test bed, a fuse can be tested about every 15 min, which is primarily dependent on the fuse setup time. This needs to be compared with the manufacturing time of a HFCG (roughly 8–16 man hours) and the explosive test setup time (2-3 h). These are considerable time and cost savings that enable varying fuse geometries/materials in a wider range than ever possible with a purely HFCG driven fuse test scheme. After successful fuse optimization with the test bed, the optimized fuse design will be directly transferred to a HFCG based pulsed power source for HPM generation.

IV. SUMMARY

The nonexplosive test bed system for helical flux compression generator fuse testing shows a reliable, repetitive system capable of up to a 45 kA output. The total stored energy of the system is 5.6 kJ and is utilized for fuse vaporization events similar to the use of a HFCG. The pulse forming network is the basis of the system and by utilizing a free wheeling diode assembly is expected to have a long operating lifetime. By using magnetic switches in the changing inductance method, the overall cost is significantly reduced and exhibits low system maintenance. Furthermore, with the PSPICE modeling, easy and accurate results for future fuse design can easily be accomplished via simulation in place of experimentation. By utilizing the nonexplosive test bed along with the PSPICE modeling, a faster and more accurate

method for fuse testing for the HFCG units has been established.

- Opening Switches, Advances in Pulsed Power Technology (1989), Vol. 1.
- ⁵ Opening Switches, Advances in Pulsed Power Technology, edited by A. Guenther, M. Kristiansen, and T. Martin (Plenum, New York, 1987).
- ⁶Explosively Driven Pulsed Power, Helical Flux Compression Generators, edited by A. Neuber (Springer, Berlin, 2005).
- ⁷G. N. Glasoe and J. V. Lebacoz, *Pulse Generators* (Dover, New York, 1965).
- ⁸W. C. Nunnally, *Magnetic Switches and Circuits*, Pulsed Power Lecture Series (Lecture No. 25) (Texas Tech. University, Lubbock, TX, 1981).

¹ A. Neuber and J. Dickens, Proc. IEEE **92**, 1205 (2004).

²J.-C. Hernandez, A. Neuber, J. Dickens, and M. Kristiansen, *IEEE Transactions*, Special Issue of IEEE Trans. Plasma Sci. **32**, 1902 (2004).

³ M. Giesselmann, T. Heeren, E. Kristiansen, J. G. Kim, J. C. Dickens, and M. Kristiansen, IEEE Trans. Plasma Sci. 28, 1368 (2000).

⁴R. E. Reinovsky, Fuse Opening Switch for Pulsed Power Applications,